

# **ScienceDirect**

FAC Papers Online

IFAC PapersOnLine 58-28 (2024) 372-377

# Enhancing Traffic Flow via Feedback Linearization and Model Predictive Control under Input Constraints

Arash Rahmanidehkordi\* Amirhossein Ghasemi\*

\* Department of Mechanical Engineering, University of North Carolina at Charlotte, Charlotte, NC, USA (e-mail: arahmani@charlotte.edu, ah.qhasemi@charlotte.edu)

#### Abstract:

This paper introduces a novel algorithm that combines feedback linearization (FL) with model predictive control (MPC) for managing highway traffic as an over-actuated, constrained nonlinear system. FL converts the non-linear traffic flow dynamics of the METANET model into a linear form, but it does not inherently handle control command constraints. To address this, an MPC will be integrated that takes the linearized output from the FL controller and produces the virtual control commands for the FL controller. Followed by that, a novel constraint mapping algorithm will be presented to determine these virtual control commands, ensuring all input constraints are met. The algorithm also selects the most cost-effective command for optimal reference tracking. Simulations validate the approach, showing significant improvements in traffic flow and reductions in average travel times.

Copyright © 2024 The Authors. This is an open access article under the CC BY-NC-ND license (https://creativecommons.org/licenses/by-nc-nd/4.0/)

 $\label{lem:control} \textit{Keywords:} \ \text{Feedback Linearization, METANET, Traffic Control, Model Predictive Control, Constraint Mapping}$ 

### 1. INTRODUCTION

The average American driver lost 36 hours to congestion in 2021, costing \$564 in wasted time. Pishue 2021 To address this, various traffic control approaches have been developed to reduce congestion, environmental pollution, and safety risks. These approaches cater to both urban roads and freeway networks. Hamilton et al. 2013, Siri et al. 2021 For freeway management, traffic control can be vehicle-based or road-based. Mehr and Horowitz 2019, Wang et al. 2016 Vehicle-based strategies adjust the behavior of individual vehicles, while road-based strategies influence overall traffic flow. Road-based algorithms, which are more suitable for large traffic networks, regulate flow by managing ramp entry, routing traffic, or controlling mainstream flow, often using variable speed limits (VSL). Su et al. 2014, Pasquale et al. 2017, Karimi Shahri et al. 2023

Macroscopic traffic models are essential for designing road-based controllers such as VSL. These models treat traffic as a collective entity and analyze variables such as density, speed, and flow. They can be continuous, using differential equations, Whitham 1990, Payne 1977, Lighthill and Whitham 1955, Richards 1956 or discrete, using difference equations. Daganzo 1994, Kotsialos et al. 2002 Models are also categorized by state variables: first-order models track one variable, Lighthill and Whitham 1955, Richards 1956, Daganzo 1994 while second-order models track both density and speed. Payne 1977, Kotsialos et al. 2002 The METANET model, a discrete second-order model, is widely used for freeway control and supports

various strategies, including feedback, optimal, model predictive, and advanced control frameworks. Chavoshi et al. 2023, Karimi Shahri et al. 2019, Liu et al. 2014, Ferrara et al. 2015, Chen et al. 2019

Among the various control strategies for freeway traffic, feedback controllers, such as proportional and integral (PI), or feedback linearization, stand out for their simplicity, effectiveness, and robustness in handling non-linear and uncertain traffic conditions. Müller et al. 2015, Shahri et al. 2023 These controllers adjust actions such as speed to maintain stability and prevent congestion. A critical requirement for these controllers is to consider physical constraints on control inputs, ensuring that suggested velocities are within feasible ranges and presented as discrete values for Variable Speed Limit (VSL) signs.

This paper introduces an integrated FL-MPC controller to manage freeway traffic flow. We adopt the METANET model presented in Shahri et al. 2020 and design a FL controller by measuring the density of each cell. We demonstrate that applying FL requires considering the traffic system as over-actuated to ensure full controllability under all conditions. To maintain bounded control inputs, we define the virtual control input of FL through MPC. Using the input-output linearized control (IOLC) law, we map the original input constraints to the virtual control input, creating a linear dynamical system with timevarying constraints managed by linear MPC. Chavoshi et al. 2023, Kurtz and Henson 1997 Since the proposed traffic system is overactuated, employing the common Moore-Penrose pseudoinverse in the FL process may not necessarily satisfy the constraints. The main contribution

<sup>\*</sup> This material is based upon work supported by the National Science Foundation (grant #2130704).

of this paper is addressing this limitation by proposing a novel constraint mapping algorithm that guarantees the satisfaction of the constraints. The novelty lies in exploiting the null space to generate the pseudoinverse matrix while considering the component corresponding to the optimal cost. The numerical results demonstrate that this strategy effectively improves traffic flow management.

The paper is structured as follows. Section 2 covers the METANET model for freeway traffic dynamics. Section 3 details the FL-MPC control design. Section 4 presents simulation results. Section 5 concludes and suggests future research directions.

### 2. METANET DYNAMIC

Let discretize the highway into a series of  $n_c$  cells, denoted by  $C_i$ , for  $i \in \{1, 2, \cdots, n_c\}$ . Each cell,  $C_i$ , is characterized by specific attributes, including ts length  $\ell_i$  and the number of vehicles within the cells  $n_{i,\text{veh}}$ . In this paper, to describe and control the aggregated behavior of the traffic highway, we adopt the METANET model due to its strength in analyzing and predicting traffic flow on large-scale networks. The dynamics of traffic highways can then be described with a state vector  $x = [x_1, x_2, \cdots, x_{n_c}]^T$  where for each  $i = \{1, 2, \cdots, n_c\}$ ,  $x_i = [\rho_i, v_i]^T$  represents the density  $\rho_i = n_{i,\text{veh}}/\ell_i$ , where  $n_{i,\text{veh}}$  is the number of vehicles; and the average speeds  $v_i$  within each cell  $C_i$ .

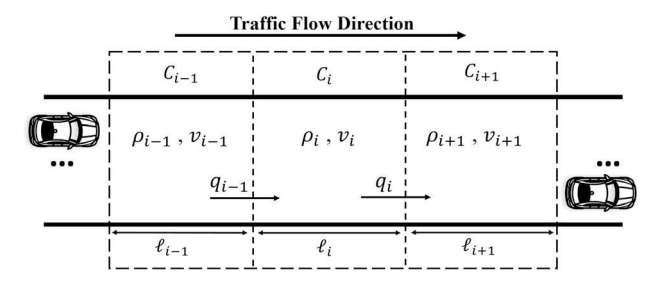


Fig. 1. Schematic of the traffic network

The changes of the density can be expressed by the conservation equation as

$$\dot{\rho}_i(t) = \frac{1}{\ell_i \gamma_i} (q_{i-1}(t) - q_i(t)) \tag{1}$$

where  $q_i(t) = \rho_i(t)v_i(t)$  is the outflows of the vehicles from the cell  $C_i$ . The changes of the average velocity in the METANET model may be expressed as

$$\dot{v}_{i}(t) = \frac{1}{\tau} \left( U_{i}(t) - v_{i}(t) \right) + \frac{1}{\ell_{i}} v_{i}(t) \left( v_{i-1}(t) - v_{i}(t) \right) - \frac{\eta}{\ell_{i} \tau} \frac{\rho_{i+1}(t) - \rho_{i}(t)}{\rho_{i}(t) + \kappa}$$

$$(2)$$

where  $U_i(t)$  is the suggested velocity to the vehicles at cell  $C_i$  at time t and  $\tau, \eta$  and  $\kappa$  are constant parameters.Lu et al. 2011 The suggested velocity  $U_i$  may be obtained as product of two terms as

$$U_i(t) = (1 - \beta_i(t))V_i(t)$$
 (3)

where  $\beta_i(t)$  is the control command and subjected to the constraint

$$0 \le \beta_i(t) \le 1 \tag{4}$$

and  $V_i(t)$  refers to the desired or target speeds that each class of vehicles aims to maintain in the absence of active

traffic control interventions, such as variable speed limits. This speed can be influenced by various factors, including traffic density, speed limits, and interaction with other vehicles class, and can be defined as

$$V_i(t) = v_{\rm ff} \exp\left[\frac{-1}{\alpha} \left(\frac{\rho_i(t)}{\rho_{{\rm cr},i}}\right)^{\alpha}\right]. \tag{5}$$

Here,  $\alpha$  is a density-dependent parameter that can be identified based on the shape of the fundamental diagram,  $v_{\rm ff}$  is the free flow velocity, and  $\rho_{{\rm cr},i}$  is the critical density of cell  $C_i$ .

It follows from (3)-(5) that the control command  $\beta_i(t)$  defined as a bounded parameter adjusts the suggested velocity of vehicles within cell  $C_i$  and ensures that the suggested velocity follows the fundamental diagram of the traffic system and therefore is reachable. In particular, it follows from (3) that in the absence of any local control command, denoted by  $\beta_i(t)=0$  the system operates without intervention, and its macroscopic dynamics conform to the steady-state velocity-density behavior. Conversely, when  $\beta_i(t)=1$  indicates that the controller recommends the vehicles come to a complete stop as per the prescribed control action.

# 3. FEEDBACK LINEARIZATION/MPC SCHEME FOR TRAFFIC MANAGEMENT

Considering n cells within the traffic network of cells from cell  $C_{i-n+1}$  to cell  $C_i$  where  $1 \leq n < n_c$  and  $i \in \{2, \dots, n_c\}$  as shown in Fig. 2. To improve the traffic flow, in this section, the goal is designing an infrastructurebased controller that calculates the suggested velocity presented to the vehicles (via adaptive speed signs) so that the density of the vehicles reaches to a desired density. In practice, the desired density feeding as a reference command to the controller can be the outcome of a higherlevel controllerKarimi Shahri et al. 2023 optimizing goals such as minimizing the total travel time, the total travel distance, or the total energy consumption. Pasquale et al. 2019 To determine the suggested velocity, a combination of FL and MPC strategies will be utilized, considering the constraint on the suggested velocity. In particular, the objective of the FL-MPC controller is to design a constrained control command  $\beta_{i,\min} \leq \beta_i \leq \beta_{i,\max}$  and make the error  $e(t) = \rho_i^d(t) - \rho_i(t)$  small. The proposed approach is described below.

#### 3.1 Feedback Linearization

The relative degree between the measured density  $y_i(t) = \rho_i(t)$  and the control command  $U_i(t)$  is two. Taking the second derivative of  $y_i = \rho_i$ , gives (for the sake of simplicity, the time (t) is not mentioned in the following equations)

$$\ddot{y}_i = \ddot{\rho}_i = f_i + [g_i \ \bar{g}_i] \begin{bmatrix} \beta_i \\ \beta_{i-1} \end{bmatrix}$$
 (6)

where

$$f_{i} = \frac{1}{\ell_{i}\gamma_{i}} (\dot{\rho}_{i-1}v_{i-1} - \dot{\rho}_{i}v_{i} + \psi_{i-1} - \psi_{i})$$

$$\psi_{i} = (\frac{\rho_{i}}{\ell_{i}} (v_{i}(v_{i-1} - v_{i}) - \frac{\eta}{\tau} \frac{\rho_{i+1} - \rho_{i}}{\rho_{i} + \kappa}) - \frac{\rho_{i}}{\tau}v_{i} + \frac{\rho_{i}V_{i}}{\tau})$$

$$g_{i} = \frac{\rho_{i}V_{i}}{\ell_{i}\gamma_{i}\tau} , \qquad \bar{g}_{i} = -\frac{\rho_{i-1}V_{i-1}}{\ell_{i}\gamma_{i}\tau}$$

$$(7)$$

As demonstrated in equation (6), an important aspect of the FL for traffic network is that there are two inputs that affect the  $\ddot{y}_i$  (i.e., inflow from the upstream cells and outflow to downstream cells). Extending equation (6) to n adjacent cells  $C_{i-n+1}$  to  $C_i$  as a block, as shown in Fig. (2), leads to

$$\ddot{\rho} = F + G\beta \tag{8}$$

where  $\beta = [\beta_{i-n}, \beta_{i-n+1}, \dots, \beta_n]^T$ , and

$$F = \begin{bmatrix} f_i \\ f_{i-1} \\ \vdots \\ f_{i-n+1} \end{bmatrix} \in \mathbb{R}^{n \times 1},$$

$$G = \begin{bmatrix} g_i & \bar{g}_i & 0 & \dots & 0 \\ 0 & g_{i-1} & \bar{g}_{i-1} & \dots & 0 \\ \vdots & & & \vdots \\ 0 & \dots & 0 & g_{i-n+1} & \bar{g}_{i-n+1} \end{bmatrix} \in \mathbb{R}^{n \times (n+1)}$$
(9)

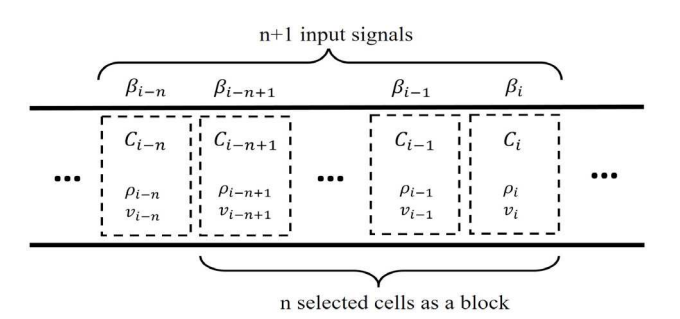


Fig. 2. Block of cells under control

The FL control command then may be expressed as

$$\beta = H \left[ -F + \nu \right] \tag{10}$$

where  $H \in \mathbb{R}^{(n+1)\times n}$  is selected such that

$$G \times H = I_n \in \mathbb{R}^{n \times n} \tag{11}$$

substituting equation (10) in (8) gives

$$\ddot{\rho} = \nu \tag{12}$$

where  $\nu = [\nu_{i-n+1}, \dots, \nu_n]^{\mathrm{T}} \in \mathbb{R}^{n \times 1}$  is the virtual decision vector defined by the designer. The conventional choice for  $\nu_i$  assumes the form  $\nu_i = \ddot{\rho}_i^{\mathrm{d}} + \xi_{1,i} (\dot{\rho}_i^{\mathrm{d}} - \dot{\rho}_i) + \xi_{0,i} (\rho_i^{\mathrm{d}} - \rho_i)$ , where  $\xi_{1,i}$  and  $\xi_{0,i}$  are constant and selected such that the output dynamics (12) be Hurwitz. However, the traditional form of  $\nu_i$  might lead to a breach of the control command constraint,  $\beta_i$ . We address this shortcoming by creation of a model predictive controller (see Section 3.2), which will facilitate the strategic selection of  $\nu$  in a manner that ensures the control command  $\beta$  remains within the defined range (i.e.  $0 \le \beta \le 1$ ).

### 3.2 Determining Virtual Commands by MPC

In this section, it will be described how a model predictive controller can be designed to determine the virtual decision vector  $\nu$  for the FL controller. First, let define a state vector  $x_{\rm mpc}$  as  $x_{\rm mpc} = [\rho_{\rm mpc} \ \dot{\rho}_{\rm mpc}]^{\rm T}$ , where  $\rho_{\rm mpc} = [\rho_i, \cdots, \rho_{i-n+1}]^{\rm T}$ . Then, the output dynamics of the FL controller expressed in equation (12) can be described as

$$\dot{x}_{\rm mpc} = A_{\rm mpc} x_{\rm mpc} + B_{\rm mpc} u_{\rm mpc} \tag{13a}$$

$$y_{\rm mpc} = C_{\rm mpc} x_{\rm mpc} \tag{13b}$$

where  $u_{\text{mpc}} = [\nu_i, \nu_{i-1}, \cdots, \nu_{i-n+1}]^{\text{T}}$  and

$$A_{\text{mpc}} = \begin{bmatrix} 0_{n \times n} & I_{n \times n} \\ 0_{n \times n} & 0_{n \times n} \end{bmatrix}, \ B_{\text{mpc}} = \begin{bmatrix} 0_{n \times n} \\ I_{n \times n} \end{bmatrix}$$

$$C_{\text{mpc}} = [I_{n \times n} 0_{n \times n}]$$

$$(14)$$

To determine  $\nu$  so that the constraint  $0 \le \beta \le 1$  on the control command can be satisfied, the following optimization is defined

$$\min_{V(k)} J = \sum_{j=0}^{N_p} \|y_{\text{mpc}}(k+j) - \rho^{d}(k+j)\|_{Q}^{2}$$
 (15)

subjected to dynamics mentioned in equation (13). Here, Q is the weight matrix, and  $N_p$  is the prediction horizon, and  $V(k) = [\nu(k|k), \cdots, \nu(k+N_u|k)]^{\mathrm{T}}$  is the decision vector with  $N_u$  being the control horizon, and  $\rho^{\mathrm{d}} = [\rho_i^{\mathrm{d}}, \cdots, \rho_{i-n+1}^{\mathrm{d}}]^{\mathrm{T}}$  is the reference signal.

Furthermore, the decision vector must satisfy  $0 \le \beta(k) \le 1$ . To develop a constraint mapping algorithm which bridges the bounds on  $\beta$  to  $\nu$ , equation (10) can be rewritten as

$$H\nu = HF + \beta \tag{16}$$

Taking the  $\beta$  bound's interval [0 1] to account gives

$$HF \le H\nu \le HF + 1 \tag{17}$$

To solve the optimization expressed in (15), several technical challenges shall be addressed. First, since both matrices F and G are state-dependent and vary with time, matrix H should be updated in real-time for all the time steps in the prediction horizon. Second, since the inequality (17) is overdetermined (i.e., H has n+1 rows but there are only n decision variables  $\nu = [\nu_1, \dots, \nu_n]^T$ ), there may not necessarily exist a solution for the constraint inequality expressed in (17). Therefore, it is essential to select a matrix H that guarantees a solution for the constraint inequality (17). A conventional choice for matrix H is to be the Moore-Penrose pseudoinverse of the input matrix G. In particular,  $H = G^{\dagger}$ , which also corresponds to the least squares solution. However, it can be shown that there is not always a solution to the inequality (17) if  $H = G^{\dagger}$ . For instance, in a case where the aim is to control the density of only one cell  $C_i$  it follows from equation (7) that  $G = [g_i \ \bar{g}_i]$ . Moreover, it is always valid that  $g_i > 0$  and  $\bar{g}_i < 0$ . The Moore-Penrose pseudoinverse of G may be represented as

$$H = G^{\dagger} = G^{T}(GG^{T})^{-1} = \begin{bmatrix} g_{i} \\ \bar{g}_{i} \end{bmatrix} ([g_{i} \ \bar{g}_{i}] \begin{bmatrix} g_{i} \\ \bar{g}_{i} \end{bmatrix})^{-1} = \begin{bmatrix} \frac{g_{i}}{g_{i}^{2} + \bar{g}_{i}^{2}} \\ \frac{\bar{g}_{i}}{g_{i}^{2} + \bar{g}_{i}^{2}} \end{bmatrix}$$
(18)

Referring to (17), the constraint for a single cell  $C_i$  in this case may be presented as

$$\frac{g_i}{g_i^2 + \bar{g}_i^2} f_i \le \frac{g_i}{g_i^2 + \bar{g}_i^2} \nu \le \frac{g_i}{g_i^2 + \bar{g}_i^2} f_i + 1 \tag{19a}$$

$$\frac{\bar{g}_i}{g_i^2 + \bar{g}_i^2} f_i \le \frac{\bar{g}_i}{g_i^2 + \bar{g}_i^2} \nu \le \frac{\bar{g}_i}{g_i^2 + \bar{g}_i^2} f_i + 1 \tag{19b}$$

dividing (19a) and (19b) by  $\frac{g_i}{g_i^2+\bar{g}_i^2}>0$  and  $\frac{\bar{g}_i}{g_i^2+\bar{g}_i^2}<0$  respectively, leads to

$$f_i \le \nu \le f_i + \frac{g_i^2 + \bar{g}_i^2}{g_i} \tag{20a}$$

$$f_i \ge \nu \ge f_i + \frac{g_i^2 + \bar{g}_i^2}{\bar{q}_i}$$
 (20b)

It follows from (20) that for  $H=G^{\dagger}$ , the intersection of the two constraint inequalities will always be the single point  $f_i$  which translates to  $\beta=0$ . Therefore,  $H=G^{\dagger}$  is not an acceptable option. The crux of this paper is to address this challenge by introducing a new constraint mapping algorithm wherein H is selected in a way that it not only satisfies (17) but also results ensures  $0 \leq \beta \leq 1$ . This challenge will be addressed in the next section where the constraint mapping algorithm is going to be discussed.

Once H is determined, by solving the mpc problem described in (15), the virtual input  $\nu$  will be obtained as the output of the MPC. Since  $\nu$  will satisfy (17), it follows from (16) that the constraint on the control command  $\beta$  will also be satisfied.

## 3.3 Constraint Mapping

To solve the previously stated problem, an algorithm is proposed which offers a set of candidate H matrices in a way that they all satisfy the inequality (17). Matrix G is a non-square matrix that always has one column more than rows. Furthermore, G is always full row rank and has a rank of n. Therefore, G always has a null space with dimension 1,  $(\dim(\mathcal{N}(G)) = 1)$ . Assuming w as a basis for the one-dimensional vector space  $(w \subset \mathcal{N}(G))$ , if matrix H satisfies the equation (11) adding any linear combination of the vector w to its column will still satisfy the equation (11), which may be articulated as

$$G(G^{\dagger} + W \Lambda) = I_n, \quad H = (G^{\dagger} + W \Lambda),$$

$$W = \begin{bmatrix} w & w & \cdots & w \end{bmatrix}, \quad \Lambda = \begin{bmatrix} \lambda_1 & 0 & \dots & 0 \\ 0 & \lambda_2 & \dots & 0 \\ \vdots & & \ddots & \\ 0 & \dots & 0 & \lambda_n \end{bmatrix}$$
(21)

where  $W \in \mathbb{R}^{n \times (n+1)}$  is a matrix whose columns are the null space basis w and  $\Lambda$  is a coefficient matrix whose elements may be chosen arbitrarily. Now, if  $\Lambda$  is chosen such that it makes the  $\hat{i}_{th}$  row of H equal to zero as

$$H_{\hat{i}} = \begin{bmatrix} h_{11}^{\hat{i}} & h_{12}^{\hat{i}} & \dots & h_{1n}^{\hat{i}} \\ \vdots & & & \vdots \\ h_{(\hat{i}-1)1}^{\hat{i}} & h_{(\hat{i}-1)2}^{\hat{i}} & \dots & h_{(\hat{i}-1)n}^{\hat{i}} \\ 0 & 0 & \dots & 0 \\ h_{(\hat{i}+1)1}^{\hat{i}} & h_{(\hat{i}+1)2}^{\hat{i}} & \dots & h_{(\hat{i}+1)n}^{\hat{i}} \\ \vdots & & & \vdots \\ h_{(n+1)1}^{\hat{i}} & h_{(n+1)2}^{\hat{i}} & \dots & h_{(n+1)n}^{\hat{i}} \end{bmatrix} \leftarrow \hat{i}_{row}^{th}$$
 (22)

then the corresponding constraint for that particular row will always be the trivial condition  $0 \le 0 \le 1$ , which is always valid, which means inequality (17) will not be overdetermined anymore. There are n+1 possible  $H_{\hat{i}} \in \{H_1, H_2, \ldots, H_{n+1}\}$  matrices with this property, where  $1 \le \hat{i} \le (n+1)$ . As  $\hat{i}_{th}$  row constraint is always satisfied, it may be removed from the  $H_{\hat{i}}$  matrix.let  $\hat{H}_{\hat{i}}$  be a square  $n \times n$  matrix which is obtained by removing the zeros row from  $H_{\hat{i}}$ , there would be n+1 candidates matrices as  $\hat{H}_{\hat{i}} \in \{\hat{H}_1, \hat{H}_2, \ldots, \hat{H}_{n+1}\}$ . Based on that, inequality (17) may be degenerated to

$$\hat{H}F \le \hat{H}\nu \le \hat{H}F + 1 \tag{23}$$

Now,  $\hat{H}$  is a full rank square matrix, which means it is invertible as well. Regarding that, range of  $\hat{H}$  will span  $R^n$ , furthermore it is always valid that  $\hat{H}F \leq \hat{H}F + 1$ , which means there is no conflict between the constraints and they are compatible. Following that, there are always feasible solutions for the MPC command vector  $\nu$ .

Now, the question that needs to be answered is, among these n+1 possible different  $H_{\hat{i}}$  matrices, which one should be considered for the constraint inequality (17). The suggested method is, before MPC makes the final decision, it will be solved once for all n+1 possible  $H_{\hat{i}}$  candidate matrices; afterward, the decision vector which attains the least cost will be applied on system and its correspondent  $H_{\hat{i}}$  matrix will be considered for the constraint (17).

Altogether, the proposed algorithm may be summarized in 5 steps:

- Step 1: Updating matrices G and F based on new states as mentioned in (7)
- Step 2: Finding w, the the single basis of  $\mathcal{N}(G)$
- Step 3: Generating the set  $H_i \in \{H_1, H_2, \dots, H_{n+1}\}$
- Step 4: Solving the MPC optimum control (15) n + 1 times for all  $H_{\hat{i}}$  set, subjected to the constraint equation (17)
- Step 5: Selecting the MPC decision vector  $\nu$  which has the least cost among the cases

To have a better understanding of the suggested algorithm, some implications may be discussed as follows. By setting a row equal to zero based on equation (21), what happens is, the corresponding  $\beta_i$  command of that cell can no longer be altered. In other words by sacrificing the redundancy we guarantee the existence of the solution for inequality (17), however, by evaluating the different possibilities we still exploit the redundancy to some extent as well.

It is important to note that the proposed algorithm is adaptable. The constraint matrices and boundaries are

state-dependent and change with time, whereas in the predictions of the MPC prediction horizon, they are considered fixed. This adaptability ensures that constraints will not be violated, a topic thoroughly investigated in Kurtz and Henson 1997

#### 4. RESULTS AND DISCUSSION

### 4.1 Numerical Simulation

The presented example includes a single-lane highway with eight road segments, all have the same length of 2 km. Cells 5 and 7 are congested and both have a density of 50 veh/km, whereas all other cells have a density of 27 veh/km. The lower bound input flow is 625 veh/h. The METANET parameters are set based on Chen et al. 2019 as shown in table (1), besides, the parameter  $\alpha$  is obtained based on the table (2) as addressed in Shahri et al. 2023 The simulation details are as follows: simulation time is 50 minutes, simulation time step is 5 seconds, MPC control period is one minute, and has the prediction horizon  $N_p = 10$  and control horizon  $N_u = 5$ . The MPC weigh matrix Q is a diagonal weight matrix with 0.1 on its diagonals. The reference signal  $\rho^{\rm d} = [\rho_i^{\rm d}, \cdots, \rho_{i-n+1}^{\rm d}]^{\rm T}$  is set to be the average of the cells' densities which is also updated with time.

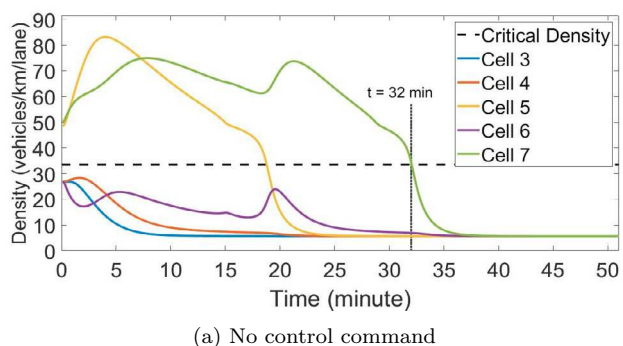
Fig. (3) and Fig. (4) demonstrate density and flow of two different cases where in the first case, there is no control command is applied to the system while in the second one, a control block including cells  $[C_7 \ C_6 \ C_5 \ C_4]$  is defined, therefore, the number of control signals would be five. As depicted in Fig. (3), applying the control command causes the congestion to be removed almost 14 minutes sooner. It is worth noting that, in the controlled case, cells  $C_3$  and  $C_4$  experience a brief period of congestion, whereas it is not the case for no-control case. It may be interpreted that the controller uses the capacity of those cells to alleviate congestion in general. Although some cells might become congested during the control period, the overall congestion time will be reduced.

Table 1. METANET Parameters

Name	Value	Unit	Name	Value	Unit
$\overline{\tau}$	18	S	$\kappa$	40	veh/km/lane
$v_{ m ff}$	110	$\mathrm{km/h}$	$ ho_{ m cr}$	33.5	veh/km/lane
$\eta$	60	$\mathrm{km}^2/\mathrm{h}$	$ ho_{ m max}$	180	veh/km/lane

Table 2. Values of Parameter  $\alpha$ 

The control efforts are demonstrated in Fig. (5). As shown in Fig. (5), all control signals for cells 3 to 7 experience changes, indicating that different constraint matrices  $\hat{H}$  have been employed throughout the simulation. Furthermore, all control commands are within the range [0 1] which proves that the proposed algorithm was successfully capable of handling the constraints. Moreover, if all the cells' densities are less than  $\rho_{\rm cr}$ , which means there is no congestion, and then all cells may reach the  $v_{\rm ff}$  speed and



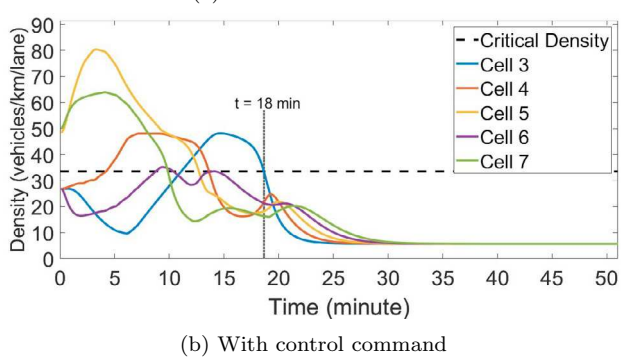
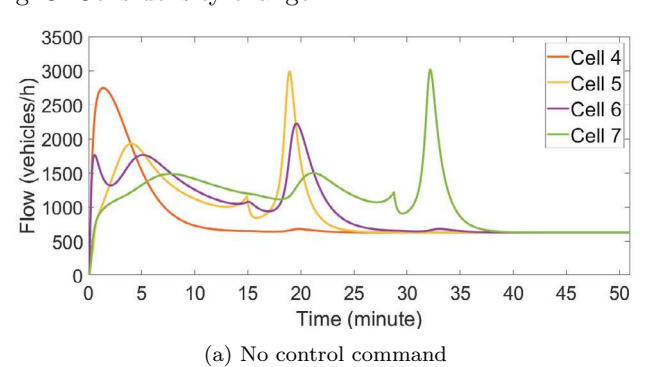
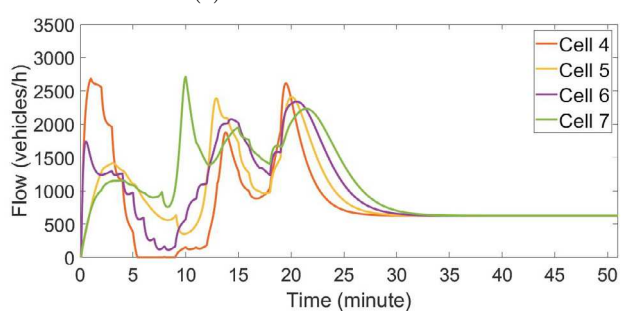


Fig. 3. Cells density change





(b) With control command

Fig. 4. Cells flow change

max possible flow, taking that into account, there is also a condition that for such cases there is no need for control command to be applied. As it may be observed in Fig. (5), after 19 minutes all commands are going to be zero which means none of the cells are in congestion anymore.

# 5. CONCLUSION AND FUTURE WORKS

This paper introduces an innovative algorithm that combines FL with MPC in order to develop a control strategy for managing highway traffic. By leveraging FL to linearize

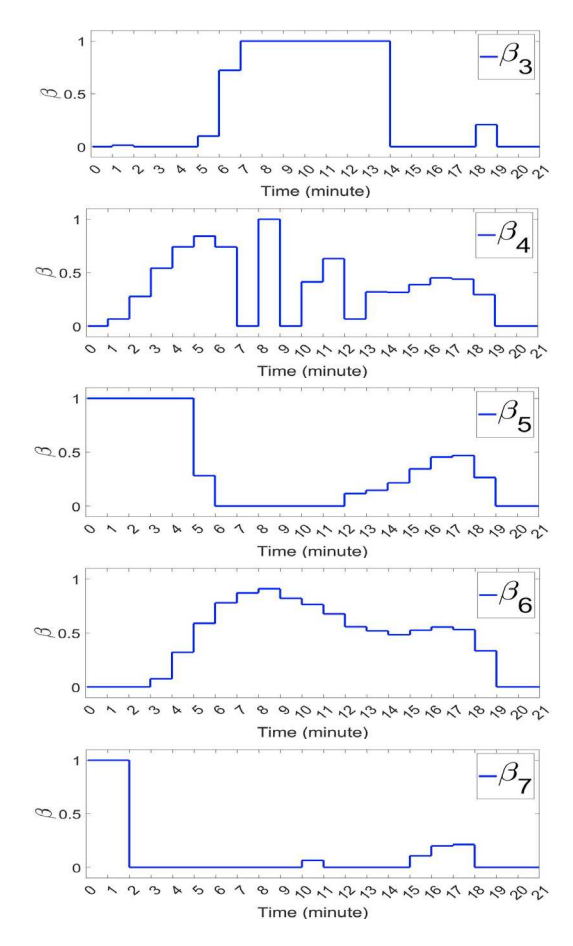


Fig. 5. Cells control effort

the nonlinear traffic flow dynamics and integrating MPC to handle constraints on control commands, the proposed method effectively addresses the challenges of controlling constrained nonlinear systems in traffic management. Also, it may be argued that by employing a nonlinear MPC technique, the constraints could be satisfied without needing a mapping algorithm. However, it should be highlighted that for cases where the aim is to control a large network of cells, the nonlinear MPC requires significant amount of computation. In contrast, solving the MPC optimization problem for the linearized system can be done in real-time, which justifies using FL.

While the results are promising, there are also issues that should be pointed out. First, the uncertainties in METANET hyperparameters need to be considered for future work. Secondly, as demonstrated, the constraint mapping algorithm can operate properly, but it considers the same set of constraints over the whole prediction horizon which is not exact because constraints are state-dependent and states are updated through the prediction steps; The same argument can be made for the references as well. This matter could cause issues, particularly with predictions for long time horizons, therefore this method will not be as accurate in such cases. This suggests a direction for future research to enhance accuracy in such scenarios.

#### REFERENCES

Hamilton, A.; Waterson, B.; Cherrett, T.; Robinson, A.; Snell, I. Transportation planning and technology 2013, 36, 24–43.

Siri, S.; Pasquale, C.; Sacone, S.; Ferrara, A. *Automatica* **2021**. *130*. 109655.

Mehr, N.; Horowitz, R. *IEEE Transactions on Control of Network Systems* **2019**, *7*, 96–105.

Wang, X.; Seraj, M.; Bie, Y.; Qiu, T. Z.; Niu, L. Journal of Transportation Engineering 2016, 142, 05016007.

Su, D.; Lu, X.-Y.; Horowitz, R.; Wang, Z. International Journal of Transportation Science and Technology 2014. 3, 179–192.

Pasquale, C.; Sacone, S.; Siri, S.; De Schutter, B. Transportation Research Part C: Emerging Technologies **2017**, 80, 384–408.

Karimi Shahri, P.; HomChaudhuri, B.; Ghaffari, A.; Ghasemi, A. H. ASME Letters in Dynamic Systems and Control 2023, 3.

Whitham, G. B. Proceedings of the Royal Society of London. A. Mathematical and Physical Sciences 1990, 428, 49–69.

Payne, H. J. Transportation Research Record 1977,

Lighthill, M. J.; Whitham, G. B. Proceedings of the royal society of london. series a. mathematical and physical sciences 1955, 229, 317–345.

Richards, P. I. Operations research 1956, 4, 42-51.

Daganzo, C. F. Transportation Research Part B: Methodological 1994, 28, 269–287.

Kotsialos, A.; Papageorgiou, M.; Diakaki, C.; Pavlis, Y.; Middelham, F. *IEEE Transactions on intelligent transportation systems* **2002**, *3*, 282–292.

Chavoshi, K.; Ferrara, A.; Kouvelas, A. Control Engineering Practice 2023, 139, 105615.

Karimi Shahri, P.; Chintamani Shindgikar, S.; HomChaudhuri, B.; Ghasemi, A. H. Optimal Lane Management in Heterogeneous Traffic Network. Dynamic Systems and Control Conference. 2019; p V003T18A003.

Liu, S.; De Schutter, B.; Hellendoorn, H. IFAC Proceedings Volumes 2014, 47, 8781–8786.

Ferrara, A.; Sacone, S.; Siri, S. Transportation Research Part C: Emerging Technologies 2015, 58, 554–567.

Chen, J.; Yu, Y.; Guo, Q. Algorithms 2019, 12, 220.

Müller, E. R.; Carlson, R. C.; Kraus, W.; Papageorgiou, M. *IEEE Transactions on Intelligent Transportation Systems* **2015**, *16*, 512–523.

Shahri, P. K.; HomChaudhuri, B.; Ghaffari, A.; Ghasemi, A. H. Infrastructure-Based Hierarchical Control Design for Congestion Management in Heterogeneous Traffic Networks. 2023 American Control Conference (ACC). 2023; pp 4399–4404.

Shahri, P. K.; Ghasemi, A. H.; Izadi, V. Optimal Lane Management in Heterogeneous Traffic Network Using Extremum Seeking Approach; 2020.

Kurtz, M. J.; Henson, M. A. Journal of Process Control 1997, 7, 3–17.

Lu, X.-Y.; Qiu, T. Z.; Horowitz, R.; Chow, A.; Shladover, S. METANET model improvement for traffic control. 2011 14th International IEEE Conference on Intelligent Transportation Systems (ITSC). 2011; pp 2148–2153.

Pasquale, C.; Sacone, S.; Siri, S.; Ferrara, A. Annual Reviews in Control 2019, 48, 312–324.